3D.1 TOWARD A CORRECTION FOR PRECIPITATION SCATTERING EFFECTS IN SATELLITE-BASED PASSIVE MICROWAVE TROPICAL CYCLONE INTENSITY ESTIMATION

Robert S. Wacker*[,1,2], Christopher S. Velden[2] and Grant W. Petty[1]
[1] Department of Atmospheric and Oceanic Science, Univ. of Wisconsin, Madison, WI
[2] Univ. of Wisconsin-Cooperative Institute for Meteorological Satellite Studies (UW-CIMSS), Madison, WI

1. INTRODUCTION

Since the late 1970s, polar-orbiting satellite microwave sounding instruments have been used to estimate tropical cyclone (TC) intensity (Kidder et al 1978, Velden and Smith 1983). The difference in microwave brightness temperature (Tb) between a TC's upper-level warm core and its environment is proportional to the MSLP anomaly associated with the TC's intensity. Currently, UW-CIMSS produces TC intensity estimates using the NOAA polar-orbiting satellite Advanced Microwave Sounding Unit-A (AMSU-A), as described in Herndon and Velden (2004). The algorithm is based on an empirically derived relationship between AMSU-A observed TC upper-tropospheric warm anomalies and coincident aircraft reconnaissance central pressure measurements.

Liquid and frozen hydrometeors in eyewall convective clouds surrounding the warm core scatter the upwelling radiance. This causes considerable variability in the observed warm core Tb's and introduces uncertainty in the resulting TC intensity estimates. This study attempts to correct for that effect.

2. THEORY

AMSU-A tropospheric sounding channels (3 through 8) are clustered near the strong 60 GHz O_2 absorption band. Higher channels have frequencies progressively closer to 60 GHz, where the atmosphere is more opaque, and are sensitive to radiance emanating from higher in the troposphere. For the furthest channels from 60 GHz (3 and 4), the atmosphere is more transparent and the underlying surface contributes a significant fraction of the observed radiance, making these channels less useful for measuring the TC's mid- to upper-level warm anomaly.

For all the AMSU-A sounding channels, absorption by water vapor and scattering by cloud droplets and small ice crystals is of little significance. However, large liquid and (especially) frozen hydrometeors scatter significantly. Since these channels are closely spaced, the frequency dependence of this scattering is small compared to its dependence on the path length traveled through the scatterers. Radiation sensed by the lower-tropospheric channels passes through a thicker layer of liquid and frozen hydrometeors, so we expect greater extinction than for the upper-tropospheric channels. The different channel-by-channel scattering effects may enable us to reduce the variability of the TC intensity estimates by selecting one subset of channels that best represents the TC warm core and another that best characterizes the scattering uncertainty.

3. DATA AND METHODOLOGY

The following results are derived from 80 AMSU-A observations of North Atlantic TC warm cores in 2003 that were nearly coincident with aircraft reconnaissance observations of TC central pressure. Half of the observations were used for training, and half for validation. For each AMSU-A observation, we estimate the TC's position by interpolating forecast track positions. We then designate the warm anomaly location as the AMSU-A field of view (FOV) containing the maximum Ch. 7 Tb within a 220 km radius of the TC position estimate. Each channel's Tb anomaly is the difference between the Tb of the warm core FOV and the mean Tb of the surrounding 30x30 FOV scene.

We used principal component analysis (PCA) to identify the leading patterns of variability in the training observations. Mathematically, PCA consists of computing the eigenvectors and eigenvalues of the covariance matrix of the observations. Each eigenvector, or empirical orthogonal function (EOF), explains a fraction of the observed variance proportional to its corresponding eigenvalue. The first EOF, associated with the largest eigenvalue, represents the multi-channel pattern responsible for most of the variability in the observations. Subsequent EOF's, which are constrained to be orthogonal to each other, explain less significant patterns of variability. Usually only the first few EOF's explain significant variance, and because of the orthogonality constraint, it is not always

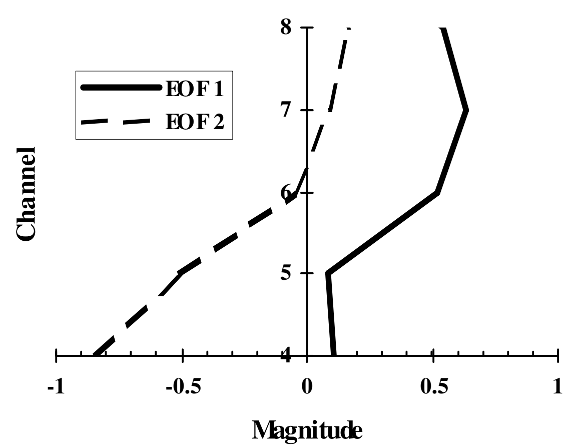

FIG. 1. First 2 EOF's (explaining 58% and 31% of variance) of TC warm core observations.

* *Corresponding author address:* Robert Wacker, UW-CIMSS, 1225 W. Dayton St., Madison, WI 53706;
e-mail: rswacker@wisc.edu.

possible to ascribe EOF's beyond the first few to physical phenomena. The projection of each observation onto the set of EOF's produces a time series of principal components (PC's) for each EOF. Each observation can then be reconstructed as a linear combination of the PC's and their corresponding EOF's.

4. RESULTS

Fig. 1 depicts the first two EOF's of the warm core observations, which explain 58% and 31%, respectively, of the observed variability. EOF1 is qualitatively similar to TC warm core vertical structure, which is maximized in the upper troposphere (Frank 1977) where channels 6-8 are most sensitive. Table 1 summarizes the root-mean-square error (RMSE) achieved by various combinations of regression predictors. Using single upper-tropospheric channels--Ch. 6, 7, or 8--results in the largest errors (RMSE near 20 hPa). PC1 is the time series of EOF1's principal components and represents magnitude of warm core signature. Using it as the sole intensity predictor offers only modest improvement (15.9 hPa RMSE) over the single-channel estimates, because PC1 is well correlated with the Ch. 6, 7, and 8 Tb anomalies. The linear-regression algorithm currently employed by CIMSS achieves better results. It examines both Ch. 7 and 8 estimates and selects the lowest resulting TC central pressure, halving the RMSE compared to using Ch. 7 or 8 alone. Note that this analysis does not incorporate an instrument scan angle bias correction employed operationally by CIMSS, which further reduces RMSE (Herndon and Velden, this volume).

TABLE 1. TC intensity estimate validation (estimate vs. reconnaissance MSLP, n=40)

Method	RMSE (hPa)
Ch6 regression	23.9
Ch7 regression	19.8
Ch8 regression	19.7
PC1 regression	15.9
CIMSS current Ch7/8 algorithm	9.5
PC1/PC2 multiple regression	9.7
CIMSS Ch7/8 with Ch5 correction	6.2
Ch8/Ch5 multiple regression	6.5

With the CIMSS Ch. 7/8 algorithm as a benchmark, we seek to further reduce estimate uncertainty by adding an additional intensity predictor to account for scattering error. EOF2 qualitatively matches the predicted scattering effect described above (decreased warm anomaly Tb for lower-tropospheric channels), so PC2 may be a good predictor of the degree of scattering. We first try a multiple regression using PC1 (warm core magnitude) and PC2 (scattering magnitude) as predictors and obtain results of comparable quality (9.7 hPa RMSE) to the CIMSS algorithm.

We achieve better performance by using the CIMSS Ch. 7/8 algorithm with a correction for scattering based on PC2. We note that PC2 is well correlated with Ch. 4 and 5 Tb anomalies. Of those two, Ch. 5 Tb anomaly is correlated best (r = -.6) with Ch. 7/8 algorithm estimate errors (Fig. 2). If we apply a scattering correction to the Ch. 7/8 algorithm using the regression relation between estimate error and Ch. 5 Tb anomaly, we reduce the RMSE to only 6.2 hPa. Finally, we achieve similar performance (6.5 hPa RMSE) by simply using Ch.8 Tb anomaly (most representative of warm core signature) and Ch. 5 Tb anomaly (most representative of scattering error) as multiple regression predictors.

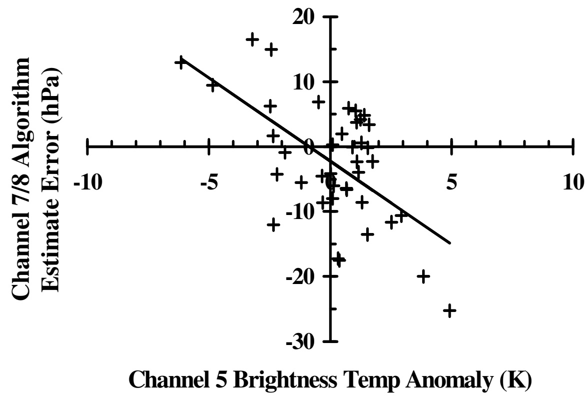

FIG. 2. CIMSS Ch. 7/8 algorithm error vs. Ch. 5 Tb anomaly. r = -.6.

5. DISCUSSION AND FUTURE WORK

Qualitative consideration of scattering effects enables us to improve the accuracy of the UW-CIMSS TC intensity estimate algorithm by employing the AMSU-A Ch. 5 Tb anomaly as an additional predictor. Future work will evaluate AMSU-A precipitation-sensing (22.8 and 31.4 GHz) and window (89 GHz) channels, as well as AMSU-B moisture-sensing channels (183.3 GHz), as scattering predictors. This work will be guided by the results of 1- and 3-dimensional simulations employing fine-scale numerical weather prediction output from TC simulation cases.

6. REFERENCES

Brueske, K.F. and C.S. Velden, 2003: Satellite-based Tropical Cyclone Intensity Estimation Using the NOAA-KLM Series Advanced Microwave Sounding Unit (AMSU). *Mon. Wea. Rev.*, **131**, 687-697.

Frank, W.M., 1977: The Structure and Energetics of the Tropical Cyclone I: Storm Structure. *Mon. Wea. Rev.*, **105**, 1119-1135.

Herndon, D.C. and C.S. Velden, 2004: Upgrades to the UW-CIMSS AMSU-based TC intensity estimation algorithm. (This volume).

Kidder, S.Q., W.M. Gray, and T.H. Vonder Haar, 1978: Estimating Tropical Cyclone Central Pressure and Outer Winds from Satellite Microwave Data. *Mon. Wea. Rev.*, **108**: 144-152.

Velden, C.S., and W.L. Smith, 1983: Monitoring Tropical Cyclone Evolution with NOAA Satellite Microwave Observations. *J. Appl. Met.*, **22**, 714-724.